

## Preparation of Flame-Retardant Membrane Materials by In-Situ Loading of $Mg(OH)_2$ on Cellulose Hydrogel from Low-Concentration $MgCl_2$ Solution

Ahmad Rokhati <sup>1</sup>, Peter Kemefa <sup>1</sup>, Luidy Arantes <sup>2,\*</sup>

<sup>1</sup> Department of Chemical Engineering, Faculty of Engineering, Diponegoro University, Semarang, 50275, Indonesia

<sup>2</sup> Rio de Janeiro State University (UERJ), Faculty of Technology (FAT), Department of Mechanical and Energy, Resende-RJ, Brazil

\*Corresponding author: luidy.arantes@fat.uerj.br

**Abstract.** This paper selects absorbent cotton as the cellulose raw material, uses a low-temperature alkaline urea solution as the dissolution system to dissolve the absorbent cotton and then regenerates it to obtain regenerated cellulose hydrogel. Lower concentration magnesium chloride solutions ( $0.01 \text{ mol}\cdot\text{L}^{-1}$ ,  $0.05 \text{ mol}\cdot\text{L}^{-1}$ ,  $0.10 \text{ mol}\cdot\text{L}^{-1}$ ,  $0.15 \text{ mol}\cdot\text{L}^{-1}$ ,  $0.20 \text{ mol}\cdot\text{L}^{-1}$ ) and sodium hydroxide solution are selected to in-situ load magnesium hydroxide onto the regenerated cellulose hydrogel through the precipitation reaction of magnesium ions and hydroxide ions. After drying, magnesium hydroxide/regenerated cellulose composite membrane materials are finally prepared. The experimental results are characterized using optical microscopy, scanning electron microscopy, and combustion performance tests. The study finds that when the absorbent cotton content is 3 wt.%, the cellulose solution concentration is moderate, facilitating uniform coating and film formation. Lower concentration in-situ loaded magnesium hydroxide has a good effect on the flame retardancy of regenerated cellulose. The reaction solution concentration significantly affects the microscopic morphology of magnesium hydroxide precipitation. When the magnesium chloride concentration is  $0.05 \text{ mol}\cdot\text{L}^{-1}$ , the precipitation loading is uniform and has nano-scale micro-protrusion structures; at concentrations of  $0.10 \text{ mol}\cdot\text{L}^{-1}$  and  $0.15 \text{ mol}\cdot\text{L}^{-1}$ , micro-prismatic flaky structures can be observed. Moreover, when the magnesium chloride reaction solution concentration is  $0.15 \text{ mol}\cdot\text{L}^{-1}$ , the theoretical loading mass fraction of magnesium hydroxide is 19.68%, the sample's average flaming time is 0 s, average glowing time is 3.83 s, and average char length is 3.83 mm, demonstrating the best flame retardant effect.

**Keywords:** Cellulose; Flame retardant modification; Magnesium hydroxide; In-situ loading; Cellulose hydrogel

Received on 15 Sep 2024, Accepted on 15 Oct 2024, Published on 15 Dec 2024

Copyright © 2024 Ahmad Rokhati *et al.* licensed to JGEEE This is an open access article distributed under the terms of the CC BY-NC-SA 4.0, which permits copying, redistributing, remixing, transformation, and building upon the material in any medium so long as the original work is properly cited.

### 1 Introduction

Cellulose, as the most abundant natural polymer on Earth, has attracted significant attention due to its renewable, biodegradable, and biocompatible properties. The strong hydrogen bonding network within cellulose molecules previously limited its applications mainly to traditional areas like textiles and paper products. However, with the rapid development of green solvent systems in recent years, particularly low-temperature alkali-urea aqueous solutions and ionic liquids, the processing and utilization of cellulose have undergone revolutionary changes. These advances have enabled the creation of various cellulose-based materials including aerogels for thermal insulation and energy storage applications, biodegradable plastics with potential to substitute petroleum-based polymers, and functional membranes for separation technologies. Despite these promising developments, the inherent flammability of cellulose remains a major obstacle for its wider application in safety-critical areas. This has stimulated extensive research on flame-retardant modifications of cellulose-based materials, with inorganic flame retardants like magnesium hydroxide emerging as particularly promising candidates due to their environmental friendliness and effectiveness [1].

The combustion behavior of cellulose involves complex thermal degradation processes that typically begin around 300°C, where cellulose chains start to break down, producing flammable gases that feed the combustion cycle. Effective flame-retardant strategies for cellulose must address multiple aspects of this process, either by interrupting the free radical reactions in the gas phase, promoting char formation to create a protective barrier, cooling the substrate through endothermic reactions, or diluting flammable gases with non-combustible volatiles. Various approaches have been developed, including internal addition during material processing, impregnation treatments, surface coating methods, and spray applications. Each method presents distinct advantages and limitations in terms of processing complexity, durability, and impact on material properties. The choice of flame-retardant method often depends on the specific application requirements and processing constraints [2].

Magnesium hydroxide has gained particular attention among inorganic flame retardants due to its excellent combination of properties, including high thermal stability, non-toxicity, and absence of corrosive gas emissions during decomposition. When heated above 340°C, magnesium hydroxide undergoes endothermic decomposition, releasing water vapor that dilutes flammable gases and cools the substrate, while the resulting magnesium oxide forms a protective char layer that acts as a thermal barrier. These multi-faceted mechanisms make magnesium hydroxide particularly effective for cellulose materials, though challenges remain in achieving uniform dispersion and maintaining the mechanical properties of the composite material at optimal loading levels [3]. The efficiency of magnesium hydroxide as a flame retardant depends significantly on factors such as particle size, distribution within the cellulose matrix, and interfacial interactions between the inorganic particles and organic polymer.

Previous research on incorporating magnesium hydroxide into cellulose matrices has evolved through several generations of approaches. Early methods focused on simple physical blending of magnesium hydroxide powder with cellulose pulp or solutions, but these often resulted in poor dispersion and significant loss of the flame retardant during processing. The work by Zhou Hui et al. demonstrated that paper treated with magnesium hydroxide-based coatings achieved flaming times of approximately 2.5 seconds and glowing times around 5 seconds, though with considerable char lengths of nearly 50 mm [4]. A significant advancement came with the development of in-situ synthesis methods, where magnesium hydroxide is precipitated directly within the cellulose matrix, leading to improved dispersion and adhesion. An Xianhui et al. pioneered the in-situ synthesis of magnesium-aluminum layered double hydroxides in paper pulp, achieving limiting oxygen index values above 25% when the deposition rate exceeded 25%, though scanning electron microscopy revealed considerable inhomogeneity in the distribution of inorganic particles on the fiber surfaces.

The field advanced substantially with the work of Han et al., who developed a sophisticated in-situ growth method for preparing magnesium hydroxide nanoparticles on cellulose hydrogel. Their approach resulted in composite aerogels that exhibited self-extinguishing behavior within 40 seconds of ignition, with significantly improved uniformity of magnesium hydroxide distribution throughout the cellulose matrix. However, their method required relatively high magnesium chloride concentrations (0.25-1.00 mol·L<sup>-1</sup>) to achieve magnesium hydroxide loadings up to 40 parts per hundred resin, which may be impractical for applications requiring specific mechanical properties or transparency [5]. The current study builds upon this foundation by exploring lower concentration ranges of magnesium chloride (0.01-0.20 mol·L<sup>-1</sup>) for in-situ precipitation of magnesium hydroxide on regenerated cellulose hydrogels, aiming to achieve effective flame retardancy with minimal additive loading.

The synthesis protocol for magnesium hydroxide/cellulose composites involves several critical stages, beginning with cellulose dissolution using environmentally friendly solvent systems. The lithium hydroxide/urea/water system has proven particularly effective, enabling molecular-level dispersion of cellulose and subsequent regeneration into hydrogels with controlled nanostructures [6]. The in-situ precipitation stage involves immersing the cellulose hydrogels in magnesium chloride solutions followed by controlled addition of sodium hydroxide, during which parameters such as concentration, temperature, and addition rate significantly influence the size, morphology, and distribution of the resulting magnesium hydroxide particles. The characterization of these composites typically employs a combination of advanced techniques, with optical and scanning electron microscopy revealing important details about the distribution and morphology of magnesium hydroxide particles within the cellulose matrix. For instance, microscopy analysis in the current study showed that at optimal magnesium chloride concentrations around 0.05 mol·L<sup>-1</sup>, magnesium hydroxide formed uniform coatings with nanoscale features, while higher concentrations led to more aggregated structures with different morphological

characteristics.

Thermogravimetric analysis provides crucial information about the thermal degradation behavior and char-forming characteristics of the composites, typically showing that magnesium hydroxide loading reduces the maximum degradation rate and increases the residual char content. Combustion testing according to standardized methods such as GB/T 14656-2009 yields quantitative data on flaming time, glowing time, and char length, with well-prepared in-situ loaded samples consistently outperforming both untreated cellulose and samples prepared by simple coating methods. The combustion results from the current study demonstrate that samples prepared with 0.15 mol·L<sup>-1</sup> magnesium chloride concentration exhibited excellent flame retardancy with zero flaming time, glowing time of 3.83 seconds, and char length of 3.83 mm, representing significant improvement over traditional coating methods and even outperforming some more complex flame-retardant systems [7].

Despite these promising results, several significant challenges remain in the flame-retardant modification of cellulose with magnesium hydroxide. The issue of uniform dispersion continues to present difficulties, as magnesium hydroxide nanoparticles tend to agglomerate, particularly at higher concentrations, leading to compromised mechanical properties and uneven flame retardancy. The optimization of loading efficiency represents another challenge, requiring careful balancing of flame-retardant effectiveness with preservation of other desirable material properties such as transparency, flexibility, and mechanical strength. The long-term durability of the flame-retardant effect under various environmental conditions, including exposure to moisture, UV radiation, and mechanical wear, requires further investigation to ensure practical applicability. Additionally, there is growing pressure to develop more environmentally friendly synthesis routes that minimize energy and water consumption while avoiding hazardous chemicals [8].

Future research directions in this field are likely to focus on several promising areas. The development of hybrid flame-retardant systems that combine magnesium hydroxide with other flame retardants, such as phosphorus or nitrogen-based compounds, could create synergistic effects that allow for lower total loadings while maintaining or even enhancing flame retardancy. Surface modification of magnesium hydroxide nanoparticles to improve their compatibility with the cellulose substrate represents another promising approach that could address dispersion challenges and enhance interfacial interactions. Advanced processing techniques, including electrospinning, 3D printing, and layer-by-layer assembly, may enable the creation of cellulose composites with tailored hierarchical structures that optimize both flame retardancy and other functional properties. There is also growing interest in developing multifunctional materials that integrate flame retardancy with additional capabilities such as antimicrobial activity, electrical conductivity, or self-healing properties, which would significantly expand the application potential of these materials.

The characterization of flame-retardant materials extends beyond basic combustion testing to include more sophisticated analyses of thermal degradation pathways and mechanisms. Thermogravimetric analysis coupled with Fourier transform infrared spectroscopy (TGA-FTIR) can provide insights into the volatile products formed during thermal degradation, helping to elucidate the gas-phase flame-retardant mechanisms. Cone calorimetry testing offers more realistic fire scenario data, including heat release rate, total heat release, and smoke production rate, which are critical for evaluating material performance in real fire conditions. Microscale combustion calorimetry provides material-level flammability parameters from small samples, enabling rapid screening of flame-retardant efficacy. These advanced characterization techniques, combined with traditional methods, contribute to a comprehensive understanding of flame-retardant mechanisms and facilitate the rational design of improved materials.

The environmental impact and sustainability aspects of flame-retardant cellulose materials deserve particular attention. While magnesium hydroxide itself is considered environmentally benign, the overall sustainability of the composite materials depends on multiple factors including the source of cellulose, the synthesis route, and the end-of-life options. Life cycle assessment studies comparing different flame-retardant strategies for cellulose-based materials are still relatively scarce but would provide valuable guidance for sustainable material development. The potential for recycling or reprocessing flame-retardant cellulose materials also requires investigation, as this could significantly influence their environmental footprint and economic viability.

In practical applications, flame-retardant cellulose materials face specific requirements depending on the intended use. For packaging materials, besides flame retardancy, properties like mechanical strength, barrier properties, and transparency may be important. For textile applications, comfort properties such as breathability, softness, and dyeability must be maintained while ensuring flame safety. In construction applications, long-term stability under various environmental conditions becomes critical. Each application area may require tailored approaches to balance flame retardancy with other functional requirements, presenting both challenges and opportunities for further research and development.

The economic aspects of producing flame-retardant cellulose materials with magnesium hydroxide also play a crucial role in their commercial viability. While magnesium hydroxide is generally less expensive than many halogenated or phosphorus-based flame retardants, the additional processing steps required for in-situ synthesis and the potential need for specialized equipment could impact production costs. Scalability of the synthesis methods from laboratory to industrial scale represents another important consideration, as many promising laboratory results face challenges when translated to large-scale production. Process optimization to minimize energy and water consumption while maximizing yield and uniformity will be essential for commercial success.

In conclusion, the in-situ loading of magnesium hydroxide on cellulose hydrogels represents a promising approach for developing eco-friendly flame-retardant materials that combine effective fire safety with environmental sustainability. The current study demonstrates that even at relatively low magnesium hydroxide loadings, significant flame-retardant improvements can be achieved through optimized synthesis conditions. By addressing the remaining challenges related to dispersion uniformity, processing scalability, and multifunctionality, such composites can find broader applications across multiple sectors including packaging, textiles, construction, and electronics. The continuous advancement in understanding fundamental mechanisms, coupled with developments in processing technologies and characterization methods, promises to accelerate the development of high-performance flame-retardant cellulose materials that meet the evolving demands of sustainable and safe material design. Future research should focus not only on enhancing flame-retardant performance but also on comprehensive sustainability assessments and development of circular economy approaches for these promising materials.

The continuous evolution of flame-retardant strategies for cellulose-based materials reflects the growing demand for sustainable alternatives to conventional petroleum-based plastics and traditional flame retardants. The unique advantage of magnesium hydroxide lies in its combination of effective flame retardancy with minimal environmental impact, particularly when compared to halogenated flame retardants that face increasing regulatory restrictions due to environmental and health concerns. The research progress in this field exemplifies a broader trend toward bio-based materials with enhanced functionality, aligning with global sustainability initiatives and circular economy principles. As understanding of nanoscale interactions between cellulose and inorganic particles deepens, and as processing technologies become more sophisticated, we can anticipate further breakthroughs in the development of cellulose-based materials that meet the dual challenges of fire safety and environmental sustainability.

The integration of flame-retardant functionality into cellulose materials represents just one aspect of the multifunctionalization trend in material science. Future developments may see the combination of flame retardancy with other properties such as sensing capabilities, energy storage functions, or adaptive responses to environmental stimuli. Such advanced materials could enable new applications in smart textiles, responsive packaging, and interactive building materials, where safety, sustainability, and functionality are equally important. The journey toward truly sustainable flame-retardant materials is complex and requires interdisciplinary collaboration across chemistry, materials science, engineering, and environmental science. The progress in magnesium hydroxide-based flame-retardant cellulose materials, as exemplified by the current study and related research, provides a solid foundation for these future advancements while addressing immediate needs for safer and more sustainable materials in various applications.

This paper sets lower concentration magnesium chloride reaction solutions to prepare magnesium hydroxide/cellulose composite membrane materials through in-situ loading on cellulose hydrogel, exploring the effect of low-concentration reaction solutions on the loading uniformity of magnesium hydroxide on cellulose hydrogel, and characterizing the flame retardancy of the composite membrane materials, to provide support for

the feasibility of low-additive magnesium hydroxide flame retardant processes for cellulose plastics.

## 2 Materials and Methods

### 2.1 Materials

Lithium hydroxide (analytical pure), urea (analytical pure), anhydrous sodium sulfate (analytical pure), absorbent cotton, sodium hydroxide (analytical pure), magnesium chloride (analytical pure).

### 2.2 Sample Preparation

#### 2.2.1 Preparation of Regenerated Cellulose Hydrogel Membrane

Place 14 g of lithium hydroxide, 24 g of urea, and 162 mL of deionized water into a 500 mL plastic beaker, stir with a glass rod until the solids are completely dissolved, then place in a freezer for 24 hours. After removal, while still cold, add a specific amount of absorbent cotton, stir until the cellulose is completely dissolved, and finally obtain a transparent viscous cellulose solution. Take a specific amount of the cellulose solution on a glass slide (75 mm × 100 mm), coat evenly with a glass rod, then immerse it in a 5 wt.% sodium sulfate aqueous solution for coagulation and regeneration. After about 10 minutes at room temperature, coagulation is complete. Carefully remove to obtain the cellulose hydrogel membrane. Wash extensively with deionized water until the pH is neutral, then set aside [9].

#### 2.2.2 In-Situ Loading of Magnesium Hydroxide

Prepare six groups of MgCl<sub>2</sub> solutions with different concentrations and corresponding molar ratios of NaOH solutions (details in Table 1). Place the washed hydrogel membranes into different concentrations of MgCl<sub>2</sub> solution (50 mL each). With ultrasonic assistance, allow Mg<sup>2+</sup> to distribute evenly in the hydrogel. Then slowly add the corresponding concentration of NaOH solution (50 mL) in batches to perform in-situ precipitation loading. White precipitate forms inside and on the surface of the cellulose hydrogel, and the hydrogel gradually changes from transparent to milky white. After the reaction is complete, carefully remove the membrane, wash extensively with deionized water until the pH is neutral. After washing, dry in an oven at 80°C for 12 hours, then seal and store. Prepare 5–7 pieces of membrane material for each group of samples.

**Table 1** Summary table of sample number, reaction solution concentration ratio, and total theoretical Mg(OH)<sub>2</sub> amount

|   | C (MgCl <sub>2</sub> mol/L) | C (NaOH mol/L) | C (Mg(OH) <sub>2</sub> mol/L) |
|---|-----------------------------|----------------|-------------------------------|
| 0 | 0                           | 0              | 0                             |
| 1 | 0.01                        | 0.02           | 0.0005                        |
| 2 | 0.05                        | 0.10           | 0.0025                        |
| 3 | 0.10                        | 0.20           | 0.005                         |
| 4 | 0.15                        | 0.30           | 0.0075                        |
| 5 | 0.20                        | 0.40           | 0.0100                        |

### 2.3 Testing and Characterization

#### 2.3.1 Sample Thickness and Precipitation Loading Amount

Use a vernier caliper to measure the thickness of the sample membranes. The theoretical loading amount of Mg(OH)<sub>2</sub> is estimated as follows.

The area of the loading glass slide is 75 mm × 100 mm, and the thickness of the hydrogel membrane is about 3 mm. Thus, the volume of each piece of cellulose hydrogel membrane is about 2.25 × 10<sup>4</sup> mm<sup>3</sup>, and the volume of the MgCl<sub>2</sub> solution is 50 mL (i.e., 5 × 10<sup>4</sup> mm<sup>3</sup>). Considering the total system volume after adding the hydrogel to the MgCl<sub>2</sub> solution becomes 7.25 × 10<sup>4</sup> mm<sup>3</sup>, assuming Mg<sup>2+</sup> is uniformly distributed throughout the system, the amount of Mg<sup>2+</sup> in the cellulose hydrogel accounts for 9/29 of the total. Therefore, for each sample, it can

be estimated that the amount of  $\text{Mg}(\text{OH})_2$  precipitated in the hydrogel is 9/29 of the total amount.

Under the same experimental conditions, the average dry mass of the 3 wt.% regenerated absorbent cotton cellulose membrane without precipitation loading is measured to be 0.554 g. Let the mass of  $\text{Mg}(\text{OH})_2$  precipitate on the membrane be  $m$ , then the loading mass fraction  $w(\text{Mg}(\text{OH})_2)$  on the regenerated cellulose membrane can be obtained by  $m/(m + 0.554 \text{ g})$ .

### 2.3.2 Distribution of $\text{Mg}(\text{OH})_2$ on Cellulose Membrane

Use an optical microscope (under ordinary transmitted light and orthogonal polarization modes) and scanning electron microscope (surface dried and gold-coated, test voltage 20 kV) to observe the loading and distribution of magnesium hydroxide in and on the surface of the membrane samples.

### 2.3.3 Combustion Performance of Sample Membranes

Place the samples under standard atmospheric conditions: temperature ( $23 \pm 1$ ) $^\circ\text{C}$ , relative humidity ( $50\% \pm 2\%$ ) for 24 hours before testing [10]. During testing, control the flame height to ( $40 \pm 2$ ) mm, directly contact the flame with the bottom end of the sample for 12 seconds, then immediately remove. Use a stopwatch to record the flaming time (the time the sample continues to burn with flame after removing the burner flame under test conditions) and the glowing time (the time the sample continues to glow after flame extinguishment under test conditions). Gently tap the charred area with a  $\Phi 6$  mm glass rod to remove loose char residue, and use a vernier caliper to measure the char length (the length of charred material that separates from the sample under test conditions) [11]. Test 5–7 samples per group, take the average of the test results, and calculate the standard deviation of the corresponding measured values for dispersion analysis. GB/T 14656-2009 states that if the test results for paper or paperboard combustion performance meet: average flaming time  $\leq 5$  s, average glowing time  $\leq 60$  s, average char length  $\leq 115$  mm, then it meets the requirements for flame-retardant paper/paperboard. Clearly, the smaller these three values, the better the flame retardancy.

### 2.3.4 Thermogravimetric Analysis of Samples

Use a thermogravimetric analyzer to analyze the thermal degradation process of the samples. Test conditions:  $\text{N}_2$  atmosphere, temperature range  $30^\circ\text{C}$ – $800^\circ\text{C}$ , heating rate  $10^\circ\text{C}/\text{min}$ .

## 3 Results and Discussion

### 3.1 Selection of Cellulose Addition Amount

In the experiment, three groups of absorbent cotton solutions with different mass fractions of 2 wt.%, 3 wt.%, and 4 wt.% were prepared. Their dissolution processes and states are shown in Figures 1b–1d.

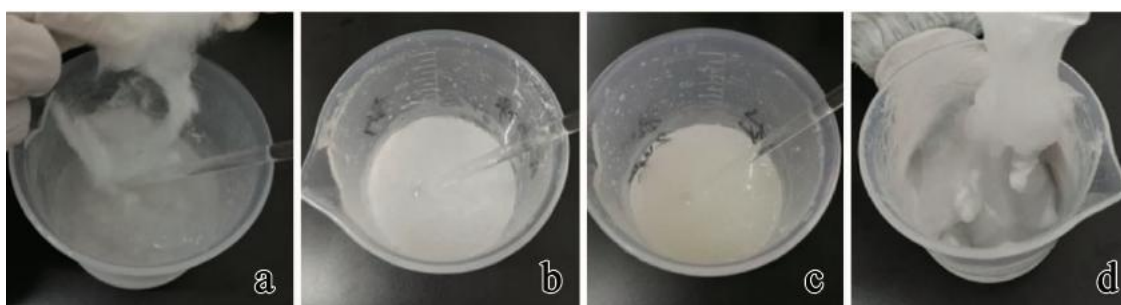


**Figure 1** Diagram of the dissolution process of absorbent cotton cellulose and the state diagram of different concentrations of absorbent cotton cellulose solution. a. Absorbent cotton fiber dissolution process; b. 2 wt.%; c. 3 wt.%; d. 4 wt.%.

Figure 1a shows the dissolution process of absorbent cotton cellulose. To ensure dissolution uniformity, the absorbent cotton needs to be torn into small pieces and added, with significant swelling of the cellulose

immersed in the solution. The 2 wt.% absorbent cotton solution dissolves quickly but has low concentration, low viscosity, and strong fluidity (Figure 1b), making it difficult to form during coating. The 4 wt.% absorbent cotton solution has too high a concentration, preventing complete dissolution of the absorbent cotton (Figure 1d), and overall dissolves slowly, has high viscosity, and strong shrinkage, making it difficult to spread and form during coating. The 3 wt.% absorbent cotton solution has moderate viscosity, as shown in Figure 1c, making it easy to control formation during coating, with good film-forming properties. Therefore, the absorbent cotton cellulose content is selected as 3 wt.%.

### 3.2 Sample Membrane Thickness and Loading Amount

The hydrogel membrane thickness is about 3 mm. After drying and loading, the thickness of all samples is < 2 mm, with varying degrees of shrinkage. From Table 2, for 0# without Mg(OH)<sub>2</sub> in-situ loading, the standard deviation S<sub>d</sub> of thickness for the six samples in the group is only 0.043, indicating high uniformity in the thickness of the prepared samples. For 1#–5#, S<sub>d</sub> increases about 7–10 times compared to 0#, indicating that precipitation loading significantly affects the within-group deviation of the final membrane sample thickness. The small differences in S<sub>d</sub> among groups 1#, 2#, and 4#, and between groups 3# and 5#, show that the reaction solution concentration does not linearly affect the thickness uniformity of the final loaded samples.

The theoretical loading mass fractions of precipitation are shown in Table 2. All samples have Mg(OH)<sub>2</sub> theoretical loading rates within 25 wt.%.

**Table 2** Sample average thickness, standard deviation, and theoretical precipitation loading rate

|   | Average thickness      |                         | Theoretical precipitation loading rate of Mg(OH) <sub>2</sub> |
|---|------------------------|-------------------------|---|
|   | Average thickness (mm) | Standard deviation (sd) |   |
| 0 | 1.14                   | 0.043                   | 0   |
| 1 | 1.50                   | 0.49                    | 1.61  |
| 2 | 1.82                   | 0.45                    | 7.55  |
| 3 | 1.26                   | 0.32                    | 14.04   |
| 4 | 1.59                   | 0.49                    | 19.68   |
| 5 | 1.88                   | 0.33                    | 24.62   |

### 3.3 Analysis of Magnesium Hydroxide Loading Situation

#### 3.3.1 Optical Microscope

From Figure 2, the 0# blank sample shows uniform light transmission, with fine cracks similar to skin surface, larger bubble-like patterns in the upper right and lower left corners, and no obvious granular dark areas. 1# and 2# show obvious granular dark areas. 3#–5# samples show significant decrease in overall light transmission, with large dark areas of different forms. 4# surface is uneven, showing irregular layers with alternating light and dark areas. This supports that as the MgCl<sub>2</sub> solution concentration increases, more Mg(OH)<sub>2</sub> is loaded onto the cellulose membrane. In 1#–5#, especially in 3#–5# samples, relatively obvious transparent areas can still be seen, indicating that the loading of Mg(OH)<sub>2</sub> in the overall regenerated cellulose membrane is very uneven.

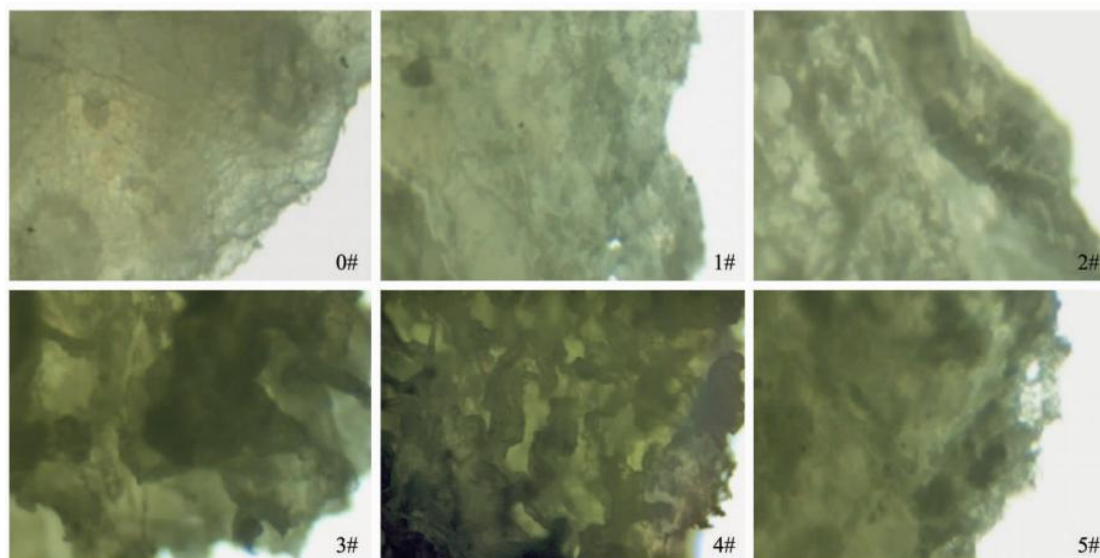


**Figure 2** Optical microscope image of cellulose sample supported by  $Mg(OH)_2$  in situ (40 $\times$ )

Select 0# and 4# for observation under orthogonal polarized light to further verify the loading situation of magnesium hydroxide inside the cellulose. From Figure 3, the 0# blank sample shows obvious light transmission, indicating high crystallinity of the unloaded regenerated cellulose membrane. For 4#, two fields of view are taken: field 1 shows strong light on the right side, field 2 shows very weak light in the middle. Compared to the blank sample, the reduction in polarized light intensity in the loaded samples should be mainly affected by magnesium hydroxide. It is visible that for the 4# sample, the loading amount and distribution of magnesium hydroxide vary at different positions. Additionally, the bright areas in the 4# sample further indicate the existence of pure cellulose micro-areas in the loaded samples. Thus, the loading of  $Mg(OH)_2$  in the overall regenerated cellulose membrane is indeed uneven.

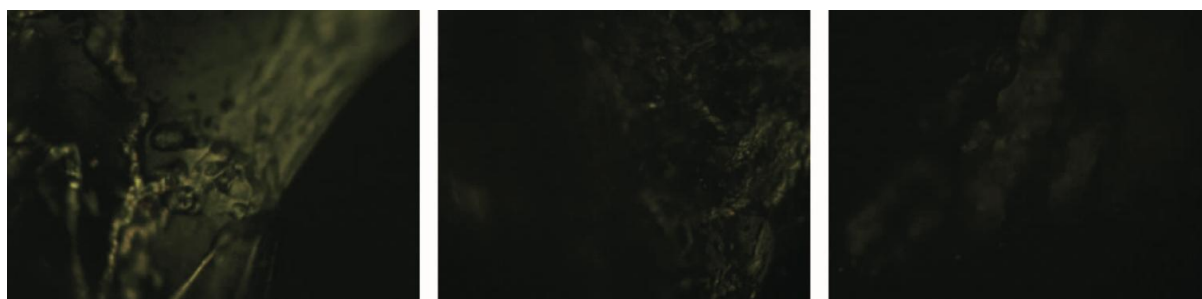


**Figure 3** Optical microscope images of 0# and 4# samples under orthogonal polarized light(40 $\times$ )

### 3.3.2 Scanning Electron Microscope

The optical microscope images show the macroscopic distribution of precipitate powder in the cellulose membrane. Further use scanning electron microscopy to observe the surface loading situation of magnesium hydroxide on the cellulose. The results are shown in Figure 4.

From Figure 4a, the surface of the dried 0# blank sample of regenerated absorbent cotton cellulose membrane has many hollow rod-like protrusion structures, with hollow gaps about 2–10  $\mu m$  in size, and tiny protrusions on flat areas. Figure 4b also has many hollow rod-like structures, with micro-protrusion structures on flat areas similar to 0#, but around the protrusion structures and on some flat surfaces, a large number of irregular microscopic particles are visible, which should be magnesium hydroxide attached to the cellulose surface [6]. From Figure 4c, the surface structure of the 2# sample is very uniform overall, with micro-protrusion diameters about 7–8  $\mu m$ , no obvious hollow pore structures, and the precipitate relatively completely coats the surface of the cellulose membrane, with nano-scale fine dots evenly distributed on the surface (details in Figure 4c1). In

Figure 4d, the 3# sample still has a few porous holes, but the hole walls are thick, surrounded by a large amount of solid magnesium hydroxide [12], and a small amount of layered flake structures can be observed [13-15] (details in Figure 4d1). In Figure 4e, the 4# surface is covered with a large amount of coating material. In the magnified view of Figure 4e1, many micro-angular structures are visible, i.e., the shape of flake or flower-ball-like magnesium hydroxide [13-15]. In Figure 4f, the 5# sample surface is covered with a large amount of irregularly shaped magnesium hydroxide [16], forming a sharp contrast with the partial loading situation on the 1# surface. Although the magnesium hydroxide coating is extensive, many holes similar to 0# are still visible, indicating poor uniformity in surface loading, and compared to 3# and 4#, the magnesium hydroxide morphology does not show obvious layered flake shapes.

Thus, increasing the  $MgCl_2$  reaction solution concentration increases the amount of precipitate coating the cellulose surface. For 2#, i.e., when the  $MgCl_2$  reaction solution concentration is  $0.05 \text{ mol}\cdot\text{L}^{-1}$ , the precipitate coating is relatively comprehensive and uniform, with some dispersed nano-scale micro-protrusion structures. From 3# to 5#, the magnesium hydroxide precipitate shows increasingly enriched situations, with layered flake magnesium hydroxide morphology visible in 3# and 4#, more obvious in 4#.

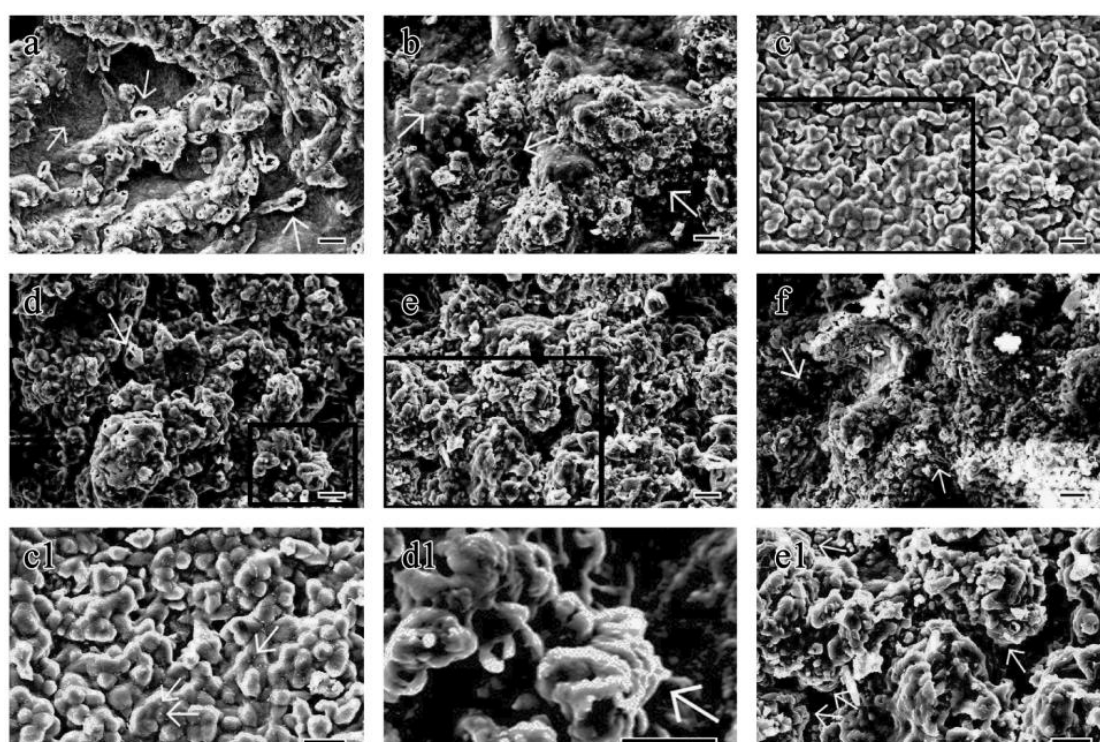


**Figure 4** a. 0#; b. 1#; c. 2#; d. 3#; e. 4#; f. 5#; c1. Partial enlargement of 2#, black box part in c; d1. Partial enlargement of 3#, black box part in d; e1. Partial enlargement of 4#, black box part in e. Bar = 20  $\mu\text{m}$

### 3.3.3 Flame Retardancy of Samples

Since each sample in each group self-extinguishes after ignition, the average flaming time  $t_f$  for each group is 0 s. The regenerated dried 0# also self-extinguishes after ignition. Under the same test conditions, if absorbent cotton is ignited, it will burn completely. This indicates that the flame retardancy of absorbent cotton cellulose improves after dissolution and regeneration. However, the average glowing time  $t_g$  for 0# is 25.83 s, with a standard deviation  $S(t_g)$  as high as 30.77, indicating that the regenerated cellulose membrane itself without loading does not have stable flame retardancy.

From Table 3, 1#, i.e., a  $MgCl_2$  reaction solution concentration of  $0.01 \text{ mol}\cdot\text{L}^{-1}$ , reduces the average glowing time and average char length of the samples by nearly 50% compared to 0#, and the standard deviations of both items significantly decrease, indicating that  $Mg(OH)_2$  loading indeed has a obvious flame retardant effect. However, at

lower concentrations, the standard deviation values are large, indicating poor stability of the flame retardant effect. Further increasing the MgCl<sub>2</sub> reaction solution concentration significantly reduces the average glowing time and average char length of the samples, but not linearly with concentration. Among them, 2# and 4# show shorter average glowing times and char lengths, with smaller corresponding standard deviations. 4# performs best with an average glowing time of 3.83 s and an average char length of 3.83 mm among all groups. The glowing time standard deviation  $S(t_g)$  for 4# is 3.06, and the char length standard deviation  $S(l)$  is 1.83, showing better stability compared to the other five groups.

Zhou Hui et al. [17] prepared flame-retardant paper using magnesium hydroxide as the flame retardant, studying the flame retardant effect of a flame retardant system mainly composed of magnesium hydroxide on paper through coating processing. The better flame retardant effect obtained with compound of magnesium hydroxide, aluminum hydroxide, ammonium polyphosphate (APP), and red phosphorus was: flaming time about 2.5 s, glowing time about 5 s, char length close to 50 mm. Clearly, the samples prepared in this experiment have superior flame retardancy compared to simple coating methods.

**Table 3** Summary table of sample combustion test results

|   | tf (s) | tg (s) | l (mm) | sd (tf) | sd (tg) | sd (l) |
|---|--------|--------|--------|---------|---------|--------|
| 0 | 0      | 25.83  | 17.17  | 0       | 30.77   | 7.54   |
| 1 | 0      | 12.71  | 9.43   | 0       | 16.75   | 4.97   |
| 2 | 0      | 6.88   | 4.62   | 0       | 4.66    | 2.24   |
| 3 | 0      | 9.43   | 7.28   | 0       | 6.87    | 3.07   |
| 4 | 0      | 3.83   | 3.83   | 0       | 3.05    | 1.81   |
| 5 | 0      | 8.57   | 5.71   | 0       | 4.95    | 1.36   |

### 3.4 Flame Retardant Mechanism Discussion

#### 3.4.1 Flame Retardant Mechanism of Unloaded Regenerated Fiber Membrane

The three elements of combustion are temperature, carbon source, and oxygen. After absorbent cotton cellulose is dissolved, regenerated, and dried into a membrane, its morphology changes from fluffy filamentous to a dense film sheet. Cellulose molecules aggregate together, greatly reducing the contact area with oxygen. Natural cellulose consists of a large proportion of crystalline regions and a smaller proportion of amorphous regions. When cotton cellulose is in its natural fiber form, its crystallinity is about 70% [17-18]. During the drying process from hydrogel to membrane, due to sufficient time and high temperature, cellulose molecules form an aggregated crystalline state, as shown in sample 0# in Figure 4. During combustion, crystalline cellulose needs to absorb heat to transform into an amorphous state, and the cellulose as a carbon source must be "thawed" from the crystal to participate in combustion. Therefore, after dissolution and regeneration, its flame retardancy is significantly improved, and the flaming time ( $t_f$ ) of each sample is 0 s.

#### 3.4.2 Flame Retardant Mechanism of Magnesium Hydroxide-Loaded Regenerated Fiber Membrane

Magnesium hydroxide primarily acts as a flame retardant through three pathways: First, magnesium hydroxide decomposes at high temperatures to produce magnesium oxide and water. This reaction is endothermic, consuming heat generated during combustion, thereby reducing the flame temperature. Second, the generated magnesium oxide is hygroscopic and can promote char formation. Third, the water produced by decomposition escapes in gaseous form, diluting flammable gases. Therefore, the loading amount and uniformity of magnesium hydroxide are the two most important factors affecting the flame retardancy of the samples. When the amount of magnesium hydroxide is appropriate and uniformly loaded, better flame retardant effects are achieved (e.g., samples 2# and 4#).

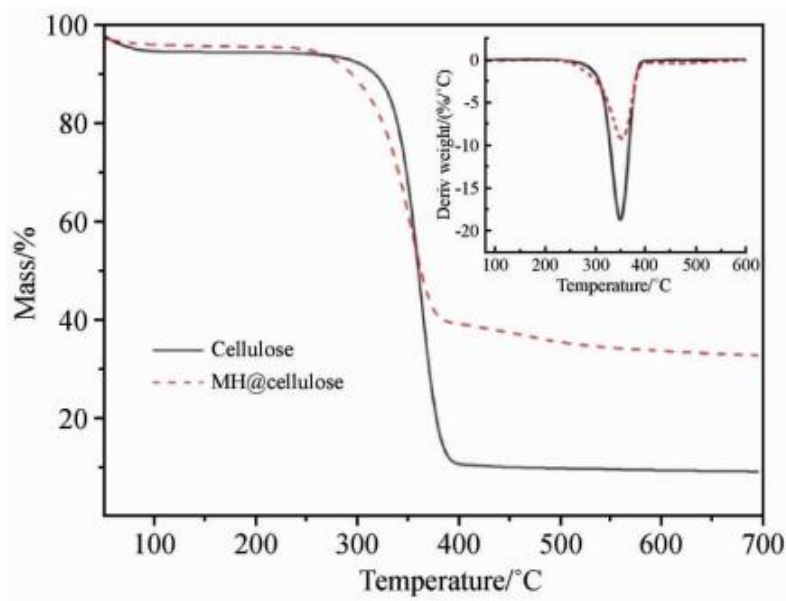


**Figure 5** TGA and DTG curves of 0# and 4# ( $c(\text{MgCl}_2) = 0.15 \text{ mol}\cdot\text{L}^{-1}$ ).

Figure 5 shows the TGA and DTG curves of the unloaded blank sample 0# and sample 4# prepared with magnesium hydroxide. It can be seen that after in-situ loading of magnesium hydroxide, the maximum thermal degradation rate of the samples is indeed reduced, and it effectively promotes carbonization of cellulose. Compared with the TG and DTG curves of the magnesium hydroxide/cellulose composite aerogel and pure cellulose aerogel prepared at a magnesium chloride reaction solution concentration of  $0.50 \text{ mol}\cdot\text{L}^{-1}$  in the study by Han et al. (Figure 5), there are some similarities and differences.

Figure 6 shows the TGA and DTG curves of neat cellulose aerogel and MH NPs@cellulose composite aerogel ( $c(\text{MgCl}_2)=0.50 \text{ mol}\cdot\text{L}^{-1}$ ) [8]. First, from the residual mass at the highest temperature, it can be seen that after in-situ loading of  $\text{Mg}(\text{OH})_2$ , the residual mass of both the aerogel and membrane samples is higher than that of their respective blanks. However, the increase rate of residual mass of the  $\text{Mg}(\text{OH})_2$ /cellulose composite aerogel prepared at a reaction solution concentration of  $0.50 \text{ mol}\cdot\text{L}^{-1}$  is much higher than that of the  $\text{Mg}(\text{OH})_2$ -loaded cellulose membrane prepared at a magnesium chloride reaction solution concentration of  $0.15 \text{ mol}\cdot\text{L}^{-1}$ . From the DTG curves of both,  $\text{Mg}(\text{OH})_2$  loading reduces the maximum thermal degradation rate of the composite samples. Similarly, the composite aerogel material shows a greater reduction. However, in terms of the numerical value of the maximum thermal degradation rate, the value for the blank cellulose aerogel is close to  $-20\%/^\circ\text{C}$ , while the maximum thermal degradation rate of the blank membrane is only close to  $-9\%/^\circ\text{C}$ . The difference in degradation rate reflects the difference in cellulose state: the aerogel has a porous structure, while the cellulose membrane is in an aggregated state. Porous structures degrade more rapidly at high temperatures. Moreover, from the DTG curves, it can be seen that the absolute decomposition rate above  $300^\circ\text{C}$  for the loaded samples is lower than that of their respective blanks. In the loaded aerogel, the DTG peak is a sharp single peak, and the temperature corresponding to the maximum thermal degradation rate is higher than that of the blank aerogel. This indicates that for the aerogel, the loading of  $\text{Mg}(\text{OH})_2$  on cellulose is relatively uniform and can synchronously act as a flame retardant promoting carbonization, reducing the thermal degradation rate of cellulose and increasing the temperature corresponding to the maximum thermal degradation rate. In the loaded cellulose membrane, the DTG peak is very broad and exhibits an obvious double peak, and the temperature corresponding to the maximum thermal degradation rate is lower than that of the blank membrane. The distinct double peak indicates poor uniformity of magnesium hydroxide loading on cellulose in the composite membrane state. With uneven loading, a considerable portion of magnesium hydroxide decomposes without acting on the cellulose, decomposing first on its own. After self-decomposition, the original positions of magnesium hydroxide become pores in the fiber, whereas causing the maximum thermal degradation rate temperature of the subsequent cellulose part to be lower than that of the dense blank membrane material.

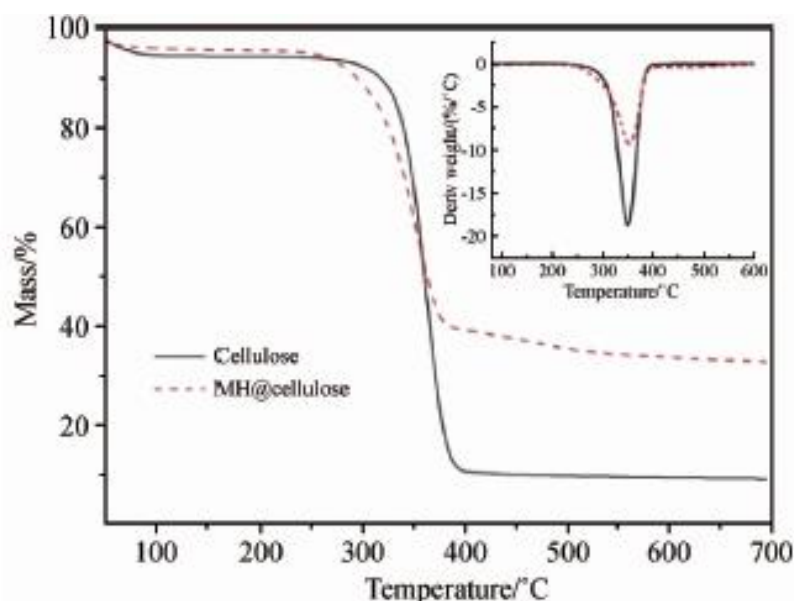


**Figure 6** TGA and DTG curves of neat cellulose aerogel and MH NPs@ cellulose composite aerogel [8]  
( $c(\text{MgCl}_2) = 0.50 \text{ mol/L}$ )

Based on the comprehensive experimental data and characterization results presented in the document, the flame-retardant mechanism of the magnesium hydroxide ( $\text{Mg}(\text{OH})_2$ )/regenerated cellulose composite membrane material is elucidated as a synergistic, multi-stage process that leverages both the altered physical state of the cellulose matrix and the chemical actions of the in-situ precipitated inorganic filler. The mechanism begins with the intrinsic flame retardancy imparted to the cellulose itself after dissolution in the LiOH/urea system and subsequent regeneration into a hydrogel followed by drying. This process transforms the fluffy, high-surface-area absorbent cotton fibers into a denser, aggregated film-like state, as confirmed by SEM images showing a consolidated structure. This morphological change significantly reduces the material's contact area with atmospheric oxygen, a crucial element for combustion. Furthermore, during the drying process, cellulose molecules have sufficient time and thermal energy to reorganize, increasing the crystallinity of the regenerated membrane. As evidenced by the optical microscopy under polarized light (Figure 3), the unloaded sample (0#) exhibited high crystallinity. Crystalline cellulose requires additional thermal energy to undergo a "melting" or disordering transition from a crystalline to an amorphous state before its polymer chains can degrade into flammable volatiles, thereby acting as a heat sink and delaying the onset of vigorous combustion; this is reflected in the self-extinguishing behavior and zero average flaming time ( $t_f = 0 \text{ s}$ ) even for the unloaded regenerated membrane. The primary and enhanced flame-retardant action, however, is provided by the in-situ loaded  $\text{Mg}(\text{OH})_2$  particles. Upon exposure to flame or high temperature,  $\text{Mg}(\text{OH})_2$  undergoes an endothermic decomposition reaction ( $\text{Mg}(\text{OH})_2 \rightarrow \text{MgO} + \text{H}_2\text{O} \uparrow$ ), absorbing a substantial amount of heat from the immediate vicinity of the burning front, which effectively cools the substrate and retards the thermal degradation of the cellulose backbone. Concurrently, the released water vapor dilutes the concentration of oxygen and flammable pyrolysis gases (e.g., levoglucosan, furans) in the gas phase near the flame, suppressing the combustion chain reaction. In the condensed phase, the newly formed magnesium oxide ( $\text{MgO}$ ) residue serves a dual purpose: it acts as a protective, ceramic-like thermal barrier that insulates the underlying virgin material from radiant heat and oxygen ingress, and it catalyzes or promotes the char-forming reactions of cellulose. The promotion of a stable, insulating char layer is critical, as it further shields the polymer and reduces the release of flammable fuels. This char-promoting effect is directly supported by thermogravimetric analysis (TGA), which shows that the  $\text{Mg}(\text{OH})_2$ -loaded sample (4#) exhibits a higher residual mass at high temperature ( $\sim 800^\circ\text{C}$ ) compared to the unloaded blank (0#), indicating enhanced carbonization. The efficacy of this multi-faceted mechanism is highly dependent on the loading amount and, more importantly, the distribution uniformity of  $\text{Mg}(\text{OH})_2$  within the cellulose matrix. The document identifies that an optimal balance is achieved at a  $\text{MgCl}_2$  reaction solution concentration of  $0.15 \text{ mol}\cdot\text{L}^{-1}$  (sample 4#, theoretical loading of 19.68 wt.%). At this concentration, SEM analysis reveals a relatively good surface coverage with  $\text{Mg}(\text{OH})_2$  exhibiting micro-prismatic flaky morphologies, which contributes to a more effective and consistent barrier layer. This optimal morphology and distribution result in

## Preparation of Flame-Retardant Membrane Materials by In-Situ Loading of Mg(OH)<sub>2</sub> on Cellulose Hydrogel from Low-Concentration MgCl<sub>2</sub> Solution

DOI:

the best flame-retardant performance, with the sample exhibiting an average glowing time ( $t_g$ ) of only 3.83 seconds and an average char length of 3.83 mm, metrics that are vastly superior to both the unloaded regenerated cellulose and reported coating methods. The non-linear relationship between MgCl<sub>2</sub> concentration and performance (e.g., sample 5# at 0.20 mol·L<sup>-1</sup> performed worse than 4#) underscores the importance of uniformity over mere quantity; excessive or poorly distributed loading can lead to particle agglomeration, creating defects and potentially disrupting the integrity of the protective char layer. The broad and double-peaked derivative thermogravimetry (DTG) curve for the loaded membrane, compared to a sharper peak for a similar aerogel system referenced, further corroborates the challenge of achieving perfectly uniform dispersion in the dense membrane structure. In summary, the superior flame retardancy stems from a combined physical barrier effect from densified cellulose, an endothermic cooling and fuel-diluting action from Mg(OH)<sub>2</sub> decomposition, and the formation of a reinforced MgO-char composite layer, with the overall efficiency dictated by the nano/micro-scale dispersion and interfacial interactions between the inorganic particles and the organic biopolymer network.

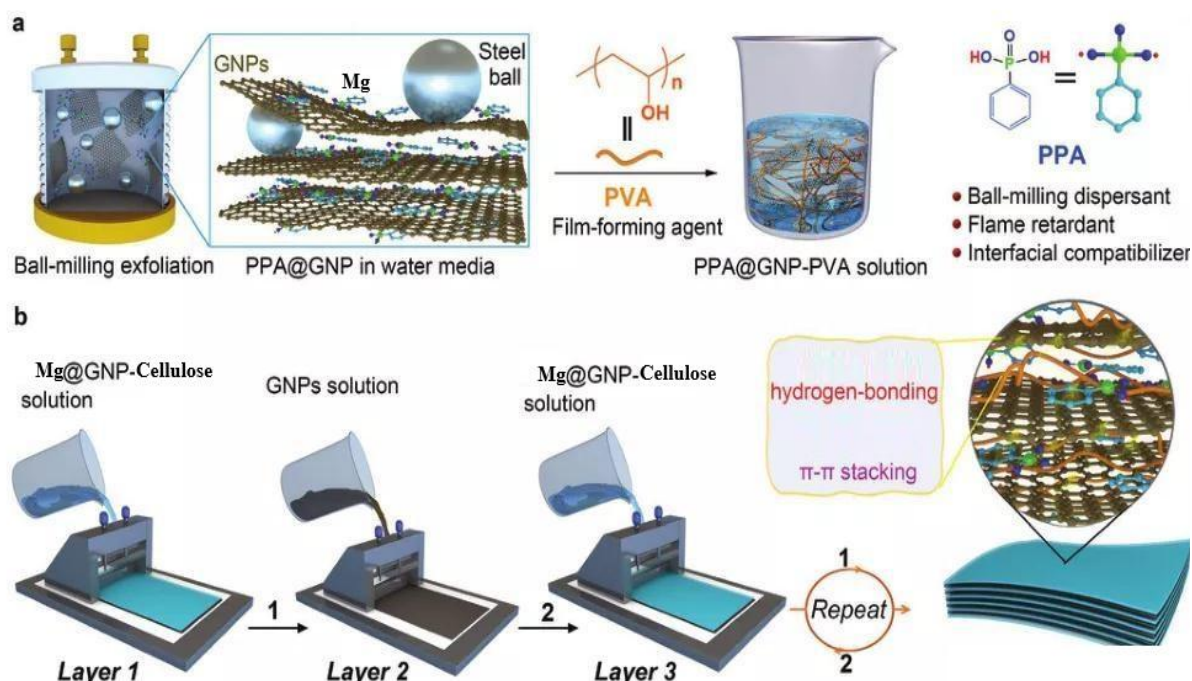


**Figure 7** Proposed flame retardant mechanism

Based on the experimental findings presented in this document, the future application prospects for the Mg(OH)<sub>2</sub>/regenerated cellulose composite membranes are particularly promising in sectors demanding both high fire safety and environmental sustainability, leveraging the material's effective, non-toxic, and bio-based nature. The study demonstrates that even with a relatively modest and theoretically optimized loading (19.68 wt.% at 0.15 mol·L<sup>-1</sup> MgCl<sub>2</sub>), the composite achieves excellent self-extinguishing behavior with minimal afterglow and char length, outperforming traditional coating methods. This positions the material as a strong candidate for next-generation, eco-friendly flame-retardant barriers. A primary application lies in sustainable packaging, especially for electronics, luxury goods, or documents, where the composite film could serve as a protective, flame-resistant interlayer or pouch that aligns with circular economy principles due to its cellulose backbone. In the construction and interiors sector, these membranes could be integrated as surface laminates or coatings for insulation materials, furniture, or decorative panels, providing an added layer of fire safety without relying on halogenated compounds. The textile industry represents another key area; the in-situ loading process could be adapted to treat regenerated cellulose fibers (like lyocell) or fabrics, creating inherently flame-retardant clothing for professions with high thermal risk or for home furnishings such as curtains and upholstery. Furthermore, the technology holds potential for specialty papers and filtration membranes used in electrical insulation or industrial settings where flammability is a concern. Future development must focus on overcoming the key challenge of improving the distribution uniformity of Mg(OH)<sub>2</sub> within the dense cellulose matrix, as indicated by

the broad DTG peaks and optical microscopy. Advancements in hydrogel processing, perhaps through controlled drying or the use of dispersing agents, will be crucial to enhance performance consistency and mechanical properties. Scaling the in-situ precipitation process from laboratory batches to continuous, roll-to-roll production will be essential for commercial viability. Research may also explore the development of multifunctional composites by co-precipitating  $\text{Mg}(\text{OH})_2$  with other benign additives (e.g., clay nanosheets, phosphorus compounds) to create synergistic effects, potentially lowering the total inorganic loading required while adding properties like improved mechanical strength or antimicrobial activity. Ultimately, the successful translation of this research could provide a viable, scalable pathway for manufacturing cellulose-based materials that meet stringent fire safety standards without compromising on environmental and health criteria, contributing significantly to the replacement of conventional, less sustainable plastics and flame retardants in a wide array of applications.

## Conclusion

(1) When the addition amount of absorbent cotton is 3 wt.%, the cellulose solution concentration is moderate, facilitating easy coating and film formation.

(2) The distribution of the precipitate is significantly affected by the reaction solution concentration, and the overall uniformity is poor.

(3) Different magnesium chloride reaction solution concentrations have a significant impact on the crystal morphology of magnesium hydroxide. When the magnesium chloride reaction solution concentration is  $0.05 \text{ mol}\cdot\text{L}^{-1}$ , the surface loading of magnesium hydroxide is the most uniform and has micro-nano scale protrusion structures. At concentrations of  $0.10 \text{ mol}\cdot\text{L}^{-1}$  and  $0.15 \text{ mol}\cdot\text{L}^{-1}$ , micro-prismatic flaky [19] morphologies are observed on the loaded membrane surface, and at a concentration of  $0.15 \text{ mol}\cdot\text{L}^{-1}$ , the amount of flaky morphology is greater.

(4) In-situ loading of magnesium hydroxide has a significant effect on the flame retardant modification of regenerated cellulose membranes. When the magnesium chloride reaction solution concentration is  $0.15 \text{ mol}\cdot\text{L}^{-1}$ , the theoretical loading mass fraction is 19.68%, the surface distribution uniformity of magnesium hydroxide precipitate is the best, the average flaming time of the sample is 0 s, the average glowing time is 3.83 s, and the average char length is 3.83 mm, demonstrating the best flame retardant effect.

(5) The cellulose membrane prepared by in-situ loading of magnesium hydroxide has significantly improved flame retardancy compared to samples with direct coating of inorganic flame retardants [7]. By performing in-situ loading of lower concentration magnesium hydroxide on the regenerated hydrogel obtained after cellulose dissolution and regeneration, cellulose can be well flame-retardant modified. However, the uniformity of magnesium hydroxide loading inside the cellulose membrane needs further improvement.

## References

- [1] CHEN Yanguo, LI Zhiwei, LI Xiaohong, et al. Preparation and flame retardancy of cellulose/graphene oxide composite aerogel [J]. *China Plastics*, 2019, 33(1): 33-39.
- [2] WANG Qiyang. Construction, structure and properties of a new type of cellulose bioplastic [D]. Wuhan: Wuhan University, 2014.
- [3] WEI Wei. Study on preparation process and flame retardant properties of high-efficiency halogen-free flame retardant paper [D]. Fuzhou: Fujian Agriculture and Forestry University, 2017.
- [4] AN Xianhui, QIAN Xueren, LONG Yufeng. Preparation of flame retardant paper based on in-situ synthesis of magnesium-aluminum layered double hydroxides [J]. *China Pulp & Paper*, 2007(8): 1-5.
- [5] SHI Ran, TAN Liwen, CHENG Lingling, et al. Preparation and characterization of flame retardant modified cellulose pulp and flame retardant paper [J]. *Polymer Materials Science & Engineering*, 2017, 33(1): 142-147.
- [6] NING Zhiqiang, ZHAI Yuchun, GU Huimin, et al. Preparation of magnesium hydroxide from boron mud [J]. *Mining and Metallurgical Engineering*, 2008(2): 60-62.

- [7] ZHOU Hui, LIU Zhong, WEI Yajing. Study on preparation of flame retardant paper with magnesium hydroxide as flame retardant [J]. *China Pulp & Paper*, 2009, 28(1): 13-16.
- [8] HAN Y Y, ZHANG X X, WU X D, et al. Flame retardant, heat insulating cellulose aerogels from waste cotton fabrics by in situ formation of magnesium hydroxide nanoparticles in cellulose gel nanostructures [J]. *ACS Sustainable Chemistry & Engineering*, 2015, 3(8): 1853-1859.
- [9] CHEN, Y., WANG, S., LIU, H., et al., 2023. Optimization of operational parameters for Ag/Bi<sub>2</sub>WO<sub>6</sub> photocatalytic degradation of antibiotics. *Chemical Engineering Journal*, 454, 140345.
- [10] LI, X., HANG, K., WANG, Y., et al., 2022. Construction of 3D hierarchical Ag/Bi<sub>2</sub>WO<sub>6</sub> microspheres for efficient photocatalytic degradation of antibiotics. *Chemical Engineering Journal*, 435, 134892.
- [11] WANG, Q., LIU, J., CHEN, H., et al., 2024. Defect engineering of Ag/Bi<sub>2</sub>WO<sub>6</sub> for enhanced photocatalytic degradation of fluoroquinolone antibiotics. *Chemical Engineering Journal*, 485, 149872.
- [12] WU Zhiming, ZHANG Hongbang, SONG Lei, et al. Preliminary study on the formation mechanism of high magnesium scale during continuous production of magnesium hydroxide [J]. *Inorganic Chemicals Industry*, 2019, 51(10): 77-80.
- [13] WU Yun, MA Zhen, CHEN Jie, et al. Preparation and dispersion control of magnesium hydroxide [J/OL]. *Journal of Wuhan Institute of Technology*, 2020, 42(4): 429-433 [2020-08-10]. <https://doi.org/10.19843/j.cnki.CN42-1779/TQ.201907021>
- [14] ZHU Huayang, ZHONG Jianchu, YU Benru, et al. Controlled synthesis of spherical magnesium oxide [J/OL]. *Inorganic Chemicals Industry*, 2020, 52(11): 33-36 [2020-08-10]. <http://kns.cnki.net/kcms/detail/12.1069.TQ.20200509.1626.008.html>
- [15] WU Yufei, CHANG Shufeng, YANG Guoying. SEM analysis of particle size and microscopic state of magnesium hydroxide [J]. *Journal of Chinese Electron Microscopy Society*, 2001, 20(4): 312-313.
- [16] FAN Chonghui, WANG Haiyang, XU Yang. Preparation and properties of magnesium hydroxide self-assembled high-efficiency flame retardant cotton fabric [J]. *New Chemical Materials*, 2019, 47(8): 106-109+114.
- [17] LIU Jie, ZHANG Yuzhong, GAO Peiji, et al. Study on the supermicrostructure of natural cellulose by scanning tunneling microscopy [J]. *Journal of Chinese Electron Microscopy Society*, 1997, 16(6): 41-44.
- [18] ZHANG Yanan, XU Shengnan, JI Fan, et al. AFM single molecule recognition study of cellulose degradation [J]. *Journal of Chinese Electron Microscopy Society*, 2020, 39(4): 377-382.
- [19] CAO Fengze, YAN Peiyu. Research progress on hydration characteristics and microstructure of hydration products of concrete expansion agent [J]. *Journal of Chinese Electron Microscopy Society*, 2017, 36(2): 187-193.